GEOPHYSICAL RESEARCH LETTERS, VOL. 25, NO.11, PAGES 1907-1910, JUNE 1, 1998

Wet and dry sizes of atmospheric aerosol particles: An AFM-TEM study

Mihály Pósfai[1,2], Huifang Xu[1,3], James R. Anderson[1], and Peter R. Buseck[1]

Abstract. We studied the hygroscopic behavior of atmospheric aerosols by using a novel approach, the combination of atomic force microscopy (AFM) with transmission electron microscopy (TEM) imaging of the same individual particles. By comparing the dimensions of hydrated and dry ammonium sulfate particles collected above the North Atlantic Ocean, we determined that particle volumes are up to four times larger under ambient conditions (as determined by AFM) than in the vacuum of a transmission electron microscope. We interpret these changes as resulting from the loss of water. Organic films on the particles may be responsible for the relatively large water uptake at low relative humidities.

Introduction

Hygroscopic growth of atmospheric aerosol particles affects their light-scattering properties and their ability to become cloud condensation nuclei (CCN) (Pilinis et al., 1995; Quinn et al., 1996; Tang, 1996). Owing to small compositional differences, the hygroscopic properties of synthetic and natural particles can differ. For example, about 6% of the mass of sea-salt particles is water at 30% relative humidity (RH), whereas pure NaCl is essentially dry (McInnes et al., 1996). Submicrometer aerosol particles at the Grand Canyon contain acidic organics that enhance water vapor condensation (Zhang et al., 1993); on the other hand, in an urban atmosphere (Los Angeles) organic species diminish water uptake by inorganics (Saxena et al., 1995). Thus, the composition-dependent hygroscopic properties of natural aerosols can be best understood if the compositions of specific species are known and if individual, ambient aerosol particles are studied.

Electron-beam instruments are commonly used tools for individual-particle studies (Sheridan et al., 1993; Pósfai et al., 1995). The two-dimensional morphology of an aerosol particle can be observed using TEM, once the particle is trapped on a grid; however, its thickness can be only estimated, and in the vacuum of the electron microscope the adsorbed water is lost.

Atomic force microscopy (AFM) provides quantitative information about particle sizes in three dimensions (Blum, 1994). To our knowledge, only one AFM study has been performed on environmental aerosol samples (Friedbacher et al., 1995). The advantage of AFM over electron-beam techniques is that it is performed under ambient conditions, so there is no risk of modifications of the particles by a vacuum or an electron beam. We used TEM for studying the same particles for which we collected AFM data. Thus, we studied the morphologies of particles under ambient conditions (by AFM), then obtained information about compositions and structures of the same particles (by TEM) after they were dried in the vacuum of the TEM.

Experimental Techniques

Aerosol samples were collected during the Atlantic Stratocumulus Transition Experiment/Marine Aerosol and Gas Exchange (ASTEX/MAGE) experiment in the North Atlantic (Huebert et al., 1996). Particles were collected directly onto formvar-coated Cu TEM grids placed on the fourth stage of a Casella cascade impactor. The fourth stage of the impactor samples particles with aerodynamic diameters 0.2 to 0.7 μm. Temperature, RH, wind speed, and the results of TEM analyses of individual particles collected on the third stage of the impactor are given by Pósfai et al. (1995). The samples used for this study were collected June 19, 1992 from 11:37 to 15:47 (sample #1) and June 20, from 09:58 to 14:04 (sample #2), when a polluted air mass of European origin was sampled.

The TEM grids with the collected aerosol particles were placed in the center of a steel disc, which was placed on the AFM sample stage. A Digital Instrument NS-III AFM was used for imaging in the contact mode in air. A square-shaped object (a microchip) with 10 μm-long edges was used for calibrating image dimensions; we found that the images are stretched by 14% along the direction of scanning relative to the direction perpendicular to it. The images obtained from aerosol particles were corrected for this distortion.

We used a JEOL 2000FX TEM operated at a 200-kV accelerating voltage and equipped with a double-tilt (±30°; ±45°) goniometer stage. In the column of the TEM the vacuum is c. 10^{-6} torr. TEM images were used to observe particle morphologies, their structures were identified using selected-area electron diffraction (SAED), and elemental compositions were determined by energy-dispersive X-ray spectrometry (EDS); experimental details are given by Pósfai et al. (1995).

Results

Low-magnification AFM and TEM images of identical areas of sample #1 (Figs. 1a and 1b, respectively) reveal that the same particles can be observed using the two methods. EDS analyses combined with SAED patterns show that all particles are $(NH_4)_2SO_4$, with the majority containing soot aggregates. While $(NH_4)_2SO_4$ is very beam-sensitive in the TEM, at sufficiently low beam currents (< 5 pA/cm^2, as measured on the viewing screen) the particles can be observed without

[1]Departments of Geology and Chemistry/Biochemistry, Arizona State University, Tempe, Arizona.
[2]Department of Earth and Environmental Sciences, University of Veszprém, Veszprém, Hungary.
[3]Current address: Department of Earth and Planetary Sciences, University of New Mexico, Albuquerque, New Mexico.

Paper number 98GL01416.
0094-8534/98/98GL-01416$05.00

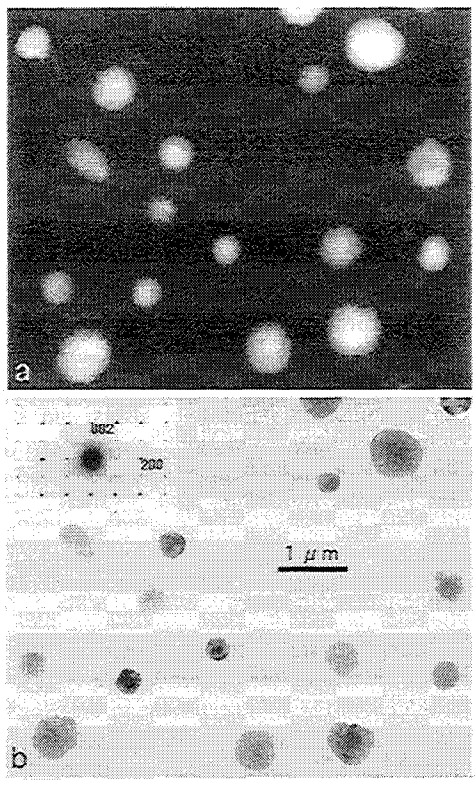

Figure 1. Low-magnification AFM (a) and TEM (b) images of an identical area in sample #1. The inset in the upper-left corner of (b) is an SAED pattern obtained from one of the particles; it indicates that the particle is a single crystal of $(NH_4)_2SO_4$. The non-uniform contrast of the particles in (b) is caused by diffraction effects.

destroying them. Even though the particles are round, most are single crystals of $(NH_4)_2SO_4$ (see the SAED pattern in Fig. 1b); a smaller number are aggregates of several crystals.

Particle dimensions can be measured directly from higher resolution AFM images (Fig. 2a) and cross-sectional profiles (Fig. 2b). For example, particle A has an average diameter of 1.6 μm at its base, and its height is 0.32 μm, as measured by the vertical distance between the two arrows that mark the base and top of the particle. From the AFM data the volumes of particles A and B were calculated to be 0.40 and 0.41 μm^3, respectively. For this calculation we fitted a parabolic curve to the AFM profile of the particle and, on the basis of AFM images, we regarded the particle rotationally symmetric around a vertical axis through its center. Assuming original spherical shapes and no volume changes during and after sample collection, the diameters of the original airborne particles were 0.8 and 0.9 μm. The particles have a characteristic bumpy surface structure (Fig. 2a) that is suggestive of a polycrystalline substance; perhaps the particles recrystallized in the TEM into single crystals of $(NH_4)_2SO_4$.

TEM images (Figs. 2 c,d) show the same particles as in Figure 2a. In Figure 2c they have not yet suffered damage in the electron beam, whereas Figure 2d shows them in the process of evaporation. Soot aggregates (marked X and Y) within or on the edges of the $(NH_4)_2SO_4$ particles remain unchanged in the beam. Faint halos around the particles appear in both TEM images; they are more distinct in Fig. 2d, where one is partly marked by the dashed line (lower left).

The diameters of the halos around particles in the TEM images are the same as the particle diameters obtained from the AFM image (Fig. 2a). The soot particles can be used as orientation points when the AFM and TEM images are compared. Soot aggregates marked X stick out as far as the outer edges of the halos (Fig. 2d); they can also be observed in the AFM image (Fig. 2a), bulging out from the surface of the sulfate particle. On the other hand, the soot particles marked Y are inside the halos and cannot be seen in the AFM image, indicating that they were enclosed when the AFM scan was performed. The diameters of particles (as measured at their bases) decreased by 20(±5)% in the vacuum, as indicated by the difference between AFM and TEM particle sizes and also by the same difference between the diameters of halos and particles in the TEM images (Fig. 2d). Assuming that particle heights also shrink by 20(±5)%, the dimensional changes translate into a volume decrease of about 36(±8)% for both particles A and B. These observations indicate that the particles lost mass, presumably water, in the vacuum of the TEM.

We performed a series of experiments with sample #2. First an AFM scan of selected sample areas and particles was performed. Then the sample was inserted into the TEM vacuum for five minutes but, in order to avoid beam damage, the electron beam was not turned on. After the sample was removed from the vacuum and exposed to the ambient RH (31%) for two hours, a second AFM scan followed. Finally, the particles were analyzed using the TEM.

A series of images obtained in the three experiments (AFM before vacuum, AFM after vacuum, TEM) are shown in Figure 3. In the AFM images the particles are slightly elongated along the direction of scanning, which is from W to E in (a) and from

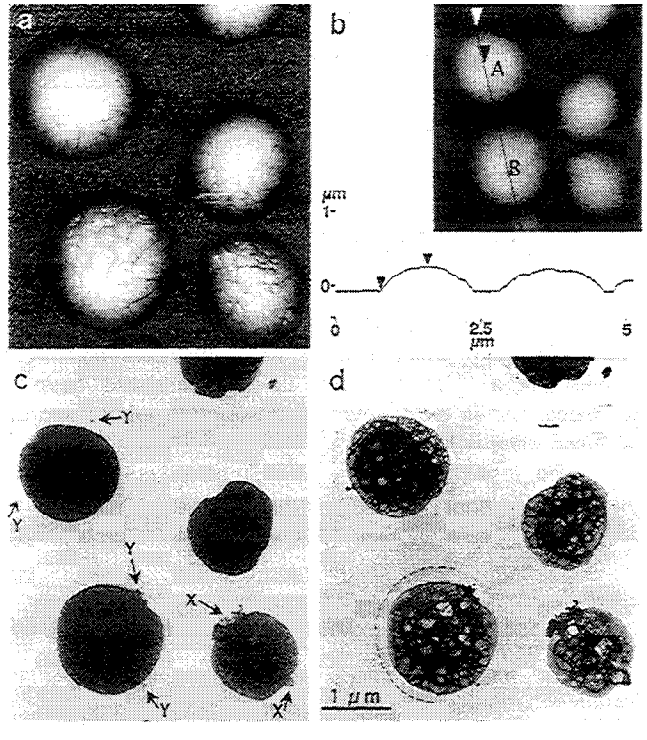

Figure 2. AFM image (a), cross-sectional profile (b), and TEM images (c,d) obtained from the same four $(NH_4)_2SO_4$ particles from sample #1. X and Y mark soot aggregates. Halos are visible around the particles in (d); one is marked by the dashed line. See text for discussion.

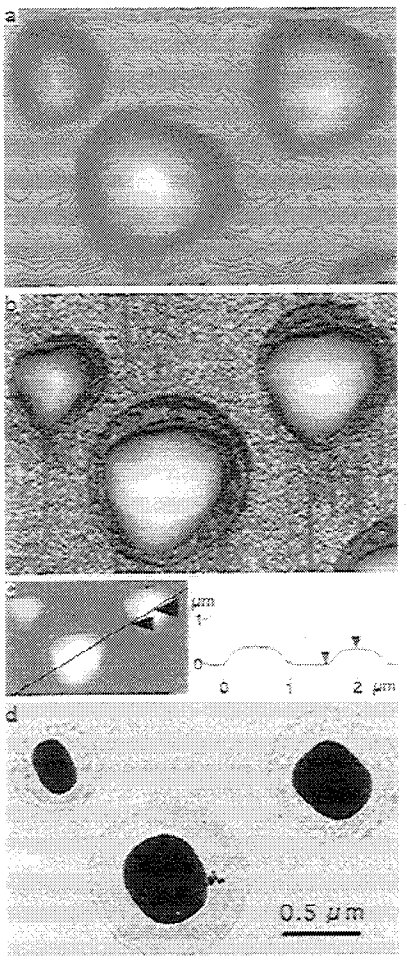

Figure 3. (a) AFM image of original particles in sample #2; (b) AFM image and (c) cross-sectional profile of the same particles after they were exposed to high-vacuum conditions; (d) TEM image of the same particles. See text for explanation.

N to S in (b,c); we believe that the elongated shapes result from capillary effects between the scanning tip and the thick water layer on the particles. Even with the uncertainty caused by the apparent changes in morphologies, particle sizes obtained in the three experiments can be compared and the original and dry volumes of particles can be determined with reasonable accuracy. In the TEM (d), sample #2 looks similar to sample #1 because it also contains $(NH_4)_2SO_4$ particles with soot cores.

The sequence of changes in particle sizes in our experiment can be best understood if the images in Figure 3 are studied in the order (a), (d), (b), and (d). The apparent TEM diameters of dry particles are 40(±5) to 50(±5)% smaller than those of the original particles (measured with AFM at their bases, parallel to the collection surface). If we assume that the particles shrink in the vacuum but their shapes do not change significantly, then a 50% decrease in diameter means a 75% loss of volume. (Here again the volume calculation is based on the AFM profile of the particles.) Particles in (b) have intermediate sizes. The AFM image clearly shows halos around them; apparent particle diameters are about 25(±5)% smaller than halo diameters. The fact that the particles grew significantly after removal from the vacuum indicates that they equilibrated at the ambient RH (31%) by adsorbing moisture from the air.

Discussion

The accuracy of particle dimensions obtained from AFM data depends on instrumental parameters such as scanning speed, magnification, and tip geometry. Artifacts can lead to larger apparent diameters than the actual values; however, the measured particle heights are unaffected. The apparent diameter of a particle should be regarded as the upper limit of the real diameter. The good agreement between particle diameters (as seen by AFM) and halo diameters (as seen by TEM) in Figure 2 indicates that any artificial enlargement of horizontal particle dimensions by the AFM is less than 5%. For comparison, these diameters are roughly twice as large as of airborne particles, assuming that such particles would have spherical shapes and volumes identical to those that we studied by AFM.

Our results indicate that the studied sulfate particles contain large amounts of volatile species, presumably water. This high water content can result from the presence of acidic sulfate in the particles, organic films on their surfaces, or the combined effects of both.

At the time of sample collection, the RH was 79 and 65% for samples #1 and #2, respectively; under such conditions, sulfate particles are usually deliquesced solution droplets (Rood et al., 1989). During dehydration, a particle may stay in a metastable liquid phase until the RH drops below the spontaneous dehydration point, at which time crystallization takes place (Chen, 1994). Since the studied particles may have been exposed to variable humidities during storage, we cannot know whether the sizes observed with the AFM were in equilibrium with the ambient air or the particles were in a metastable, deliquesced state. However, when sample #2 was put into the vacuum, the particles dehydrated; therefore, we know that after removal from the vacuum these particles were in the stage of hygroscopic growth and had equilibrated at ~31% RH when they were studied for the second time with the AFM. The two types of AFM experiments, one on "pre-vacuum" particles with unknown hydration histories and the other on "after-vacuum" particles, provide different information regarding the particles and are discussed here separately.

NH_4HSO_4 and particularly H_2SO_4 particles contain water even at low (<40%) RHs (Hoppel et al., 1996). Bulk aerosol analyses during ASTEX/MAGE (Zhuang and Huebert, 1996) indicate that the ratio of NH_4^+/SO_4^{2-} was about unity when our samples were collected. It is possible that the particles were still acidic when the first AFM scan was performed; their acidity may be responsible, at least in part, for their large (up to 3/4 of their volumes) water content. The acid content of the particles could have been protected during storage by organic coatings; thin organic films on H_2SO_4 droplets are known to retard both the neutralization of acid and the evaporation of water from the particles (Däumer et al., 1992).

Our SAED patterns show that once in the TEM, all particles were crystalline $(NH_4)_2SO_4$, most with soot inclusions. In the vacuum of the TEM there is no possibility for the particles to retain a liquid coating that could contain NH_4^+, SO_4^{2-}, or HSO_4^- ions; thus, after the particles were exposed to the vacuum, the hygroscopic effect of acidic sulfates, if there had been any, was no longer present. The volumes of particles in sample #2 approximately doubled (cf. Figs. 3d and 3b) two hours after removal from the vacuum. At conditions under which the last AFM scan was performed (~31% RH), pure $(NH_4)_2SO_4$ particles should presumably have been dry (Tang and Munkelwitz, 1994). It is possible that the RH of the ambient air and that

under the tip of the AFM is different; in this study we did not use an environmental cell that would have allowed us to strictly control the RH. However, even in the highly unlikely case that our RH measurement had an error as large as 20% and the RH under the AFM tip was ~50%, the doubling of the particle volume is inconsistent with a $(NH_4)_2SO_4$ composition; this large growth could only result from other components in the particles that presumably reside in their amorphous coatings.

The presence of amorphous coatings on the sulfates is strongly supported by TEM observations. When the $(NH_4)_2SO_4$ particles were evaporated with the electron beam, they left behind a residue. EDS spectra of such residues yield S, O, and C peaks; since the supporting substrate is a C-coated formvar film, we cannot determine whether the residue contains C. Although the presence of an inorganic, S-bearing amorphous coating cannot be excluded, the most feasible interpretation seems to be that the amorphous residue consists of organics. Most particles include soot, which commonly contains organic compounds in addition to elemental C (Castillo, 1986); however, the thickness of the residues does not correlate with the size of the soot inclusions, and individual soot particles (without sulfate) did not grow after removal from vacuum.

Surface-active, polar organics are abundant in atmospheric aerosols (Gill et al., 1983; Mazurek et al., 1997). Since these molecules have both a hydrophilic and a hydrophobic part, their orientations determine whether they increase or decrease the hygroscopicity of the coated aerosol particle (Andrews and Larson, 1993). Organic compounds have been shown to form cloud condensation nuclei (Cruz and Pandis, 1997) and to alter the growth of inorganic salt droplets (Shulman et al., 1996). We believe our "after-vacuum" AFM observations are suggestive of particle-size changes resulting from the hygroscopic effects of organic coatings on the sulfates.

Conclusions

Our study shows that AFM and TEM methods can be successfully combined for studying atmospheric aerosol particles. The three-dimensional morphological information obtained using AFM is complemented by compositional and crystallographic information obtained using TEM. Accurate particle volumes can be determined from AFM data; from these, the original, "airborne" diameters can be calculated. Different particle sizes obtained with the two methods indicate that sulfate particles lose volatile species, most likely water, in the vacuum of the TEM. It is likely that coatings of organic compunds on the particles are responsible for the observed anomalies in the hygroscopic behavior of sulfates. We plan to extend our AFM studies by using an environmental cell for obtaining more quantitative data on the hygroscopic behavior of natural particles at controlled and variable RH conditions.

Acknowledgments. We thank Herman Sievering for providing the aerosol samples and two anonymous reviewers for their helpful comments. This research was supported by grant ATM-9408704 from the Atmospheric Chemistry Division of the NSF. Electron microscopy was performed using equipment at the Center for High-Resolution Electron Microscopy at Arizona State University.

References

Andrews, E., and S. M. Larson, Effect of surfactant layers on the size changes of aerosol particles as a function of relative humidity, *Environ. Sci. Tech., 27,* 857-865, 1993.

Blum, A. B., Determination of illite/smectite particle morphology using scanning force microscopy, in *Scanning probe microscopy of clay minerals,* edited by K. Nagy and A. B. Blum, pp. 171-202, The Clay Mineral Society, Boulder, CO, 1994.

Castillo, R., An analysis of black aerosol found in two winter Atlantic coastal snow storms at Whiteface Mountain, New York, *J. Aerosol Sci., 17,* 677-684, 1986.

Chen, J.-P., Theory of deliquescence and modified Köhler curves, *J. Atmos. Sci., 51,* 3505-3516, 1994.

Cruz, C. N., and S. N. Pandis, A study of the ability of pure secondary organic aerosol to act as cloud condensation nuclei, *Atmos. Environ., 31,* 2205-2214, 1997.

Däumer, B., R. Niessner, and D. Klockow, Laboratory studies of the influence of thin organic films on the neutralization reaction of H_2SO_4 aerosol with ammonia, *J. Aerosol Sci., 23,* 315-325, 1992.

Friedbacher, G., M. Grasserbauer, Y. Meslmani, N. Klaus, and M. J. Higatsberger, Investigation of environmental aerosol by atomic force microscopy, *Anal. Chem., 67,* 1749-1754, 1995.

Gill, P. S., T. E. Graedel, and C. J. Weschler, Organic films on atmospheric aerosol particles, fog droplets, cloud droplets, raindrops, and snowflakes, *Rev. Geophys. Space Phys., 21,* 903-920, 1983.

Hoppel, W. A., G. M. Frick, and J. W. Fitzgerald, Deducing droplet concentration and supersaturation in marine boundary layer clouds from surface aerosol measurements, *J. Geophys. Res., 101,* 26,553-26,565, 1996.

Huebert, B. J., A. Pszenny, and B. Blomquist, The ASTEX/MAGE experiment, *J. Geophys. Res., 101,* 4319-4329, 1996.

Mazurek, M., M. C. Masonjones, H. D. Masonjones, L. G. Salmon, G. R. Cass, K. A. Hallock, and M. Leach, Visibility-reducing organic aerosols in the vicinity of Grand Canyon National Park: Properties observed by high resolution gas chromatography, *J. Geophys. Res., 102,* 3779-3793, 1997.

McInnes, L. M., P. K. Quinn, D. S. Covert, and T. L. Anderson, Gravimetric analysis, ionic composition, and associated water mass of the marine aerosol, *Atmos. Environ., 30,* 869-884, 1996.

Pilinis, C., S. N. Pandis, and J. H. Seinfeld, Sensitivity of direct climate forcing by atmospheric aerosols to aerosol size and composition, *J. Geophys. Res., 100,* 18,739-18,754, 1995.

Pósfai, M., J. R. Anderson, P. R. Buseck, and H. Sievering, Compositional variations of sea-salt-mode aerosol particles from the North Atlantic, *J. Geophys. Res., 100,* 23,063-23,074, 1995.

Quinn, P. K., V. N. Kapustin, T. S. Bates, and D. S. Covert, Chemical and optical properties of marine boundary layer aerosol particles of the mid-Pacific in relation to sources and meteorological transport, *J. Geophys. Res., 101,* 6931-6951, 1996.

Rood, M. J., M. A. Shaw, T. V. Larson, and D. S. Covert, Ubiquitous nature of ambient metastable aerosol, *Nature, 337,* 537-539, 1989.

Saxena, P., L. M. Hildemann, P. H. McMurry, and J. H. Seinfeld, Organics alter hygroscopic behavior of atmospheric particles, *J. Geophys. Res., 100,* 18,755-18,770, 1995.

Sheridan, P. J., R. C. Schnell, J. D. Kahl, J. F. Boatman, and D. M. Garvey, Microanalysis of the aerosol collected over south-central New Mexico during the ALIVE field experiment, May-December, 1989, *Atmos. Environ., 27A,* 1169-1183, 1993.

Shulman, M. L., M. C. Jacobson, R. J. Carlson, R. E. Synovec, and T. E. Young, Dissolution behavior and surface tension effects of organic compounds in nucleating cloud droplets, *Geophys. Res. Lett., 23,* 277-280, 1996.

Tang, I. N., Chemical and size effects of hygroscopic aerosols on light scattering coefficients, *J. Geophys. Res., 101,* 19,245-19,250, 1996.

Tang, I. N., and H. R. Munkelwitz, Water activities, densities, and refractive indices of aqueous sulfates and sodium nitrate droplets of atmospheric importance, *J. Geophys. Res., 99,* 18,801-18,808, 1994.

Zhang, X. Q., P. H. McMurry, S. V. Hering, and G. S. Casuccio, Mixing characteristics and water content of submicron aerosols measured in Los Angeles and at the Grand Canyon, *Atmos. Environ., 27A,* 1593-1607, 1993.

Zhuang, L., and B. J. Huebert, Lagrangian analysis of the total ammonia budget during Atlantic Stratocumulus Transition Experiment/Marine Aerosol and Gas Exchange, *J. Geophys. Res., 101,* 4341-4350, 1996.

J. R. Anderson, P. R. Buseck, and M. Pósfai, Departments of Geology and Chemistry/Biochemistry, Arizona State University, Tempe, AZ 85287-1404. (e-mail: mposfai@asu.edu)

H. Xu, Department of Earth and Planetary Sciences, University of New Mexico, Albuquerque, NM (e-mail: hfxu@unm.edu)

(Received July 18, 1997; revised March 2, 1998;
accepted April 9, 1998.)